SCIENCE CHINA
Information Sciences

• RESEARCH PAPER •

October 2023, Vol. 66 202202:1–202202:17
https://doi.org/10.1007/s11432-022-3701-7

Stochastic stabilization of Markovian jump systems closed by a communication network: an auxiliary system approach

Guoliang WANG[1*], Siyong SONG[1] & Chao HUANG[2]

[1]*School of Information and Control Engineering, Liaoning Petrochemical University, Fushun* 113001*, China;*
[2]*College of Information and Engineering, Northeastern University, Shenyang* 110819*, China*

Received 9 October 2022/Revised 5 December 2022/Accepted 16 January 2023/Published online 26 September 2023

Abstract This study examines the stabilization of continuous-time Markovian jump systems, whose controller is added in the diffusion section. Unlike the traditionally stochastic controllers, the proposed controller is connected by a communication network. Not only the state but also the switching signal is sampled and transmitted. Because the sampling of switching signals makes analyzing and synthesizing the system more difficult, an auxiliary system approach is presented to handle these problems. Particularly, a novel system with an exponential matrix characterizing the sampling effects is developed while the sampling rate is fully considered in the given conditions. Moreover, more special situations of sampled controllers are considered. Two numerical examples are offered to confirm the effectiveness and superiority of the methods proposed in this study.

Keywords Markovian jump system, Brownian motion, sampled switching signal, stochastic stabilization, networked control

Citation Wang G L, Song S Y, Huang C. Stochastic stabilization of Markovian jump systems closed by a communication network: an auxiliary system approach. Sci China Inf Sci, 2023, 66(10): 202202, https://doi.org/10.1007/s11432-022-3701-7

1 Introduction

A network control system (NCS) is a type of decentralized control system. It connects sensors, actuators, and controllers through a communication network. Compared with conventional control strategies, such systems [1,2] can substantially improve the efficiency, flexibility, and reliability of integrated applications. Moreover, they have the advantage of reducing installation and maintenance costs. Because of these advantages, NCSs have been rapidly developed in various fields, including remote control, air traffic control, unmanned aerial vehicles, and successful applications in automatic high-speed systems. However, the application of NCSs can have negative effects, and many results on these problems have been published, e.g., [3–8].

Furthermore, increasingly more researchers have become interested in stochastic systems because they can model many real-world systems. Many studies on stochastic systems have been published, such as [9–11]. While considering problems, the stabilization or destabilization of these systems can be realized by a stochastic controller. The designed controller is in the diffusion part and added as a Brownian noise perturbation. Based on [12], proof has been obtained that, compared with the traditional controllers in the drift section, this controller has advantages that can preserve the original state on average. When the considered system has a Markov jump property, it is natural to model it as a stochastic Markovian jump system (MJS). This special hybrid stochastic system has a wide range of applications, such as power systems, manufacturing systems, and ecosystems. Research in this area is quite extensive, and only a few references [13–17] are mentioned here. Widely investigating the existing references indicates

* Corresponding author (email: glwang@lnpu.edu.cn)

that their methods can be primarily classified into mode-dependent and mode-independent methods. In the former methods, the Markovian switching signal [18–21] should be exactly accessible, where the quantities between controllers (or filters) and original system matrices should be identical. Furthermore, the latter method [22, 23] has only one common mode and can remove the above ideal assumption. However, this method totally ignores the mode information even if it is available. Thus, it is absolute and will be conservative when the switching signal is obtained. To balance the above two methods, other control methods, such as partially mode-dependent controller [24], partial information controller [25], disordered or unmatched controller [26], scheduling controller [27], and quantity limited controller [28], have been proposed. When the stochastic MJS is mentioned, the related stochastic problems about controllers added as noise are more complicated and difficult, while the above-mentioned controllers are not applicable. Presently, few results [29–32] are available, and the related problems have not been completely studied.

Although the general cases of the stabilizing control of MJSs have been studied, some problems remain to be considered. One of these problems is the accessibility in real time of the state information of the designed controllers in the above references. This accessibility is not in accordance with NCSs in which the controlled system is connected by a communication network. In other words, the related transmitted data should be sampled before sending. When the considered system is referred to as a stochastic system, including MJSs, the stabilization problem realized by a sampling controller is not fully studied. The primary reason is that not only the system state but also the switching signal of a controller should be sampled. When a Brownian perturbation exists in MJSs, the stabilization realized by a discrete-time controller in the drift section was considered in [33]. Based on a similar method, the stochastic stabilization of stochastic systems without any jumps was examined in [12]. Although they are useful for addressing this problem, no sampling phenomenon occurs in switching signals. Very recently, the control of switched systems was considered in [34], where not only the state but also the switching signal was sampled. This approach handled the problem well for switched systems but not for MJSs. The primary reason is that an MJS's switching is determined by a Markov process, which has no minimum dwell time. When an MJS with sampled properties is examined, only a few references are available. By applying a time-scheduled Lyapunov functional approach, the stabilization of sampled-data MJSs was considered in [35, 36]. On the basis of different event-triggered schemes, control problems were studied in [37–39]. When the Markovian jump cyber-physical systems suffer randomly occurring injection attacks, the finite-time sliding mode control problem was discussed in [40]. Investigating the references for MJSs being sampled or under DoS attacks reveals that the switching signal of the abovementioned controller is not sampled. When the switching and state signals of an MJS are simultaneously sampled, an obvious but extremely difficult problem is that the sampled switching signal will be unmatched by the original Markovian switching and even no longer a Markov process. This phenomenon is not easily depicted and brings great harm to the considered system. Among the numerous references, very few of them were concerned with the above problems, and no models are available from them. All of these observations motivate the current research.

In this study, the stochastic stabilizing control of continuous-time MJSs is studied, where switching and state signals are transmitted through networks and sampled. The main contributions of this paper are as follows: (1) Unlike the stabilization on MJSs studied in [35–40], where only the state signal was sampled, a stabilizing controller with sampled switching and state signals is proposed. The phenomenon with a mismatch between original and sampled switching signals is very different from the above situations. It leads to more difficulties in system analysis and synthesis. (2) A new auxiliary model having an exponential matrix is introduced to overcome these difficulties and can characterize the sampling effects well. Furthermore, the introduction of an exponential matrix brings other problems, and novel techniques are required to address them. (3) The proposed method based on the auxiliary model is in contrast to recent results [34]. The primary difference is that the proposed event-triggered transmission scheme is very suitable for switched systems but not for MJSs because the latter switching belongs to the Markov process. Furthermore, it differs from the method in [12, 33], a robust estimation method whose sampling interval should be very small and constant. And (4) according to the proposed methods, more special applications are studied and enrich the results of MJSs. Not only the state but also the switching signal is sampled, whose advantages are illustrated by numerical examples.

Notation. n-dimensional Euclidean real spaces are represented as $\mathbb{R}^n$. The real matrices of $q \times n$ are represented as $\mathbb{R}^{q\times n}$. $(\Omega, \mathscr{F}, \mathbb{P})$ is a complete probability space. Here, Ω is the sample space, $\mathscr{F}$ is the σ-algebras of the subsets of the sample space, and $\mathbb{P}$ is the probability measure of $\mathscr{F}$. The expectation is

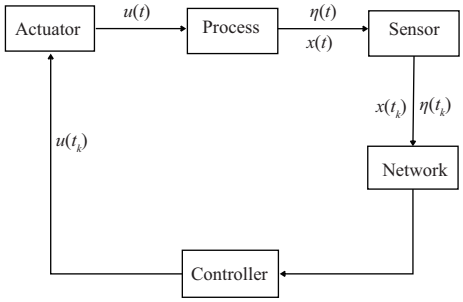

Figure 1 Diagram of system (1) closed by (3).

represented by an operator $\mathscr{E}[\cdot]$. The Euclidean vector norms or spectral norms of matrices are represented as $\|\cdot\|$. The Kronecker product and the Kronecker sum are represented by $\otimes$ and $\oplus$, respectively. The maximum eigenvalue of the symmetric matrix M is expressed as $\lambda_{\max}(M)$, and the minimum eigenvalue is expressed as $\lambda_{\min}(M)$ and $\mu_M \triangleq \lambda_{\max}\{\frac{M+M^{\mathrm{T}}}{2}\}$. A filtration$\{\mathscr{F}_t; t \in \mathbb{R}^+\}$ satisfies the usual hypotheses, that is, a right-continuous filtration augmented by all null sets in the $\mathbb{P}$-completion of $\mathscr{F}$.

2 Problem formulation

Consider a traditionally continuous time stochastic MJS defined on the complete probability space $(\Omega, \mathscr{F}, \mathbb{P})$ and described as

$$\mathrm{d}x(t) = A_{\eta(t)}x(t)\mathrm{d}t + B_{\eta(t)}u(t)\mathrm{d}\omega(t), \tag{1}$$

where $x(t) \in \mathbb{R}^n$ is the system state vector, $\omega(t)$ is a one-dimensional Brownian motion, and $u(t) \in \mathbb{R}^m$ is the control input. Matrices $A_{\eta(t)}$ and $B_{\eta(t)}$ are real constant matrices of appropriate dimensions, where $\{\eta(t), t \geqslant 0\}$ is considered a Markov chain of continuous time, and its values are obtained from the finite set $\mathscr{N} \triangleq \{1, 2, \ldots, N\}$. The transition rate matrix $\Lambda \triangleq (\lambda_{ij}) \in \mathbb{R}^{N\times N}$ is described by

$$\Pr\{\eta(t+\Delta t) = j|\eta(t) = i\} = \begin{cases} \lambda_{ij}\Delta t + o(\Delta t), & \text{if } i \neq j, \\ 1 + \lambda_{ii}\Delta t + o(\Delta t), & \text{if } i = j, \end{cases} \tag{2}$$

where $\Delta t > 0$, $\lim_{\Delta t\to 0}(o(\Delta t)/\Delta t) = 0$. When $i \neq j$, λ_{ij} is considered the transfer rate, in which the mode is i at time t. After the time interval Δt, the mode jumps to j and another one $\lambda_{ii} = -\sum_{j\neq i}\lambda_{ij}$. It is understood that conventional controllers are proposed for the above system, for example, $u(t) = K_{\eta(t)}x(t)$ and $u(t) = Kx(t)$. Here, a controller with modal and state sampling is assumed to be

$$u(t) = K_{\eta(t_k)}x(t_k), \quad t \in [t_k, t_{k+1}), \tag{3}$$

where $K_\eta(t_k)$ is the control gain to be determined, t_k is the moment of the k-th sampling and satisfies $0 = t_0 < t_1 < \cdots < t_k < \cdots$. Letting $h(t) = t - t_k$, it is calculated as $h(t) \in [0, h_k)$, $\dot{h}(t) \equiv 1$, and $h(t_k) \equiv 0$, $\forall t \in [t_k, t_{k+1})$. Moreover, it is defined that $h_k = t_{k+1} - t_k$ and $\bar{h} = \sup_{k\in\mathbb{N}}\{h_k\}$, $\forall k \in \mathbb{N}$ is the upper bound of the sampling interval. Unlike traditional Markov stabilization controllers, not only states but also modalities are sampled in controller (3). In particular, switching signals that are sampled have a noticeable negative impact on the system, and we will elaborate on this impact. In detail, because $\eta(t)$ is sampled as $\eta(t_k)$, so many combinations of switching signals occur in every interval $[t_k, t_{k+1})$. Thus, it is unreasonable or impossible to individually analyze and synthesize them. Figure 1 schematizes the changes in the system state and mode under the action of zero order holder (ZOH) after sampling.

The sampling of switching signal $\eta(t_k)$ causes considerable suffering, which makes directly analyzing closed-loop system (1) difficult. To solve the above difficulties, a new additional variable is introduced, written as $Q_i(t) = \mathscr{E}[x(t)x^{\mathrm{T}}(t)\mathbb{1}_{\{\eta(t)=i\}}]$, where

$$\mathbb{1}_{\eta(t)} = \begin{cases} 1, & \text{if } \eta(t) = i, \\ 0, & \text{otherwise.} \end{cases}$$

Then, one obtains

$$\begin{aligned}
\mathrm{d}Q_i(t) &= \mathscr{E}\left[\mathrm{d}x(t)x^{\mathrm{T}}(t)\mathbb{1}_{\{\eta(t)=i\}} + x(t)\mathrm{d}x^{\mathrm{T}}(t)\mathbb{1}_{\{\eta(t)=i\}} + x(t)x^{\mathrm{T}}(t)\mathrm{d}\mathbb{1}_{\{\eta(t)=i\}} + \mathrm{d}x(t)\mathrm{d}x^{\mathrm{T}}(t)\mathbb{1}_{\{\eta(t)=i\}}\right] \\
&= \mathscr{E}\left[A_{\eta(t)}x(t)x^{\mathrm{T}}(t)\mathbb{1}_{\{\eta(t)=i\}}\right]\mathrm{d}t + \mathscr{E}[x(t)x^{\mathrm{T}}(t)A^{\mathrm{T}}_{\eta(t)}\mathbb{1}_{\{\eta(t)=i\}}]\mathrm{d}t + \sum_{j=1}^{N}\lambda_{ji}Q_j(t)\mathrm{d}t \\
&\quad + \mathscr{E}\left[B_{\eta(t)}K_{\eta(t_k)}x(t_k)x(t_k)^{\mathrm{T}}K^{\mathrm{T}}_{\eta(t_k)}B^{\mathrm{T}}_{\eta(t)}\mathbb{1}_{\{\eta(t)=i\}}\right]\mathrm{d}t \\
&= \mathscr{E}\left[A_{\eta(t)}x(t)x^{\mathrm{T}}(t)\mathbb{1}_{\{\eta(t)=i\}}\right]\mathrm{d}t + \mathscr{E}[x(t)x^{\mathrm{T}}(t)A^{\mathrm{T}}_{\eta(t)}\mathbb{1}_{\{\eta(t)=i\}}]\mathrm{d}t + \sum_{j=1}^{N}\lambda_{ji}Q_j(t)\mathrm{d}t \\
&\quad + B_i\left\{\sum_{\ell=1}^{N}\mathscr{E}\left[K_{\eta(t_k)}x(t_k)x(t_k)^{\mathrm{T}}K^{\mathrm{T}}_{\eta(t_k)}\mathbb{1}_{\{\eta(t)=i\}}|\mathbb{1}_{\{\eta(t_k)=\ell\}}\right]p_\ell\right\}B_i^{\mathrm{T}}\mathrm{d}t \\
&= \mathscr{E}\left[A_{\eta(t)}x(t)x^{\mathrm{T}}(t)\mathbb{1}_{\{\eta(t)=i\}}\right]\mathrm{d}t + \mathscr{E}[x(t)x^{\mathrm{T}}(t)A^{\mathrm{T}}_{\eta(t)}\mathbb{1}_{\{\eta(t)=i\}}]\mathrm{d}t + \sum_{j=1}^{N}\lambda_{ji}Q_j(t)\mathrm{d}t \\
&\quad + B_i\left[\sum_{\ell=1}^{N}p_{\ell i}(h(t))K_{\eta(t_k)}x(t_k)x(t_k)^{\mathrm{T}}K^{\mathrm{T}}_{\eta(t_k)}p_\ell\right]B_i^{\mathrm{T}}\mathrm{d}t \\
&= \mathscr{E}\left[A_{\eta(t)}x(t)x^{\mathrm{T}}(t)\mathbb{1}_{\{\eta(t)=i\}}\right]\mathrm{d}t + \mathscr{E}[x(t)x^{\mathrm{T}}(t)A^{\mathrm{T}}_{\eta(t)}\mathbb{1}_{\{\eta(t)=i\}}]\mathrm{d}t + \sum_{j=1}^{N}\lambda_{ji}Q_j(t)\mathrm{d}t \\
&\quad + B_i\left\{\sum_{\ell=1}^{N}p_{\ell i}(h(t))\mathscr{E}\left[K_{\eta(t_k)}x(t_k)x(t_k)^{\mathrm{T}}K^{\mathrm{T}}_{\eta(t_k)}\mathbb{1}_{\{\eta(t_k)=\ell\}}\right]\right\}B_i^{\mathrm{T}}\mathrm{d}t \\
&= A_iQ_i(t)\mathrm{d}t + Q_i(t)A_i^{\mathrm{T}}\mathrm{d}t + \sum_{j=1}^{N}\lambda_{ji}Q_j(t)\mathrm{d}t + B_i\left[\sum_{\ell=1}^{N}p_{\ell i}\left(h(t)\right)K_\ell Q_\ell(t_k)K_\ell^{\mathrm{T}}\right]B_i^{\mathrm{T}}\mathrm{d}t \\
&= \chi_i\left(Q(t)\right)\mathrm{d}t + \vartheta_i\left(Q(t_k)\right)\mathrm{d}t,
\end{aligned} \tag{4}$$

where $\chi_i(Q(t)) = A_iQ_i(t) + Q_i(t)A_i^{\mathrm{T}} + \sum_{j=1}^{N}\lambda_{ji}Q_j(t)$, $\vartheta_i(Q(t_k)) = B_i[\sum_{\ell=1}^{N}p_{\ell i}(h(t))K_\ell Q_\ell(t_k)K_\ell^{\mathrm{T}}]B_i^{\mathrm{T}}$, $p_{\ell i}(h(t))$ indicates the probability of jumping from mode ℓ at time t to mode i after time $h(t)$, and p_ℓ is the probability that mode ℓ will occur. Its detailed computation will be given in Theorem 1.

Definition 1. Define the linear transformation operators φ, $\hat{\varphi}_i$, and $\hat{\varphi}$ in the following way: for $G = [\,G_1\ \cdots\ G_N\,] \in \mathbb{R}^{n\times Nm}$ with $G_i = [\,G_{i1}\ \cdots\ G_{im}\,] \in \mathbb{R}^{n\times m}$ and $G_{ij} \in \mathbb{R}^n$,

$$\varphi(G_i) := \begin{bmatrix} G_{i1} \\ \vdots \\ G_{im} \end{bmatrix} \in \mathbb{R}^{mn}, \quad \hat{\varphi}_i(G) := \varphi(G_i) \in \mathbb{R}^{mn}, \quad \hat{\varphi}(G) := \begin{bmatrix} \hat{\varphi}_1(G) \\ \vdots \\ \hat{\varphi}_N(G) \end{bmatrix} \in \mathbb{R}^{Nmn}.$$

Equivalently, one has

$$\varphi\left(\dot{Q}_i(t)\right) = \hat{\varphi}_i\left(\dot{Q}(t)\right) = \hat{\varphi}_i\left(\chi\left(Q(t)\right)\right) + \hat{\varphi}_i\left(\vartheta\left(Q(t_k)\right)\right), \tag{5}$$

where

$$\begin{aligned}
&\vartheta\left(Q(t_k)\right) = \left[\,\vartheta_1\left(Q(t_k)\right)\ \vartheta_2\left(Q(t_k)\right)\ \cdots\ \vartheta_N\left(Q(t_k)\right)\,\right] \in \mathbb{R}^{n\times Nn}, \\
&\chi\left(Q(t)\right) = \left[\,\chi_1\left(Q(t)\right)\ \chi_2\left(Q(t)\right)\ \cdots\ \chi_N\left(Q(t)\right)\,\right] \in \mathbb{R}^{n\times Nn}, \\
&Q_i(t) = \left[\,q_{(i-1)n+1}(t)\ q_{(i-1)n+2}(t)\ \cdots\ q_{in}(t)\,\right] \in \mathbb{R}^{n\times n}, \\
&Q(t) = \left[\,Q_1(t)\ Q_2(t)\ \cdots\ Q_N(t)\,\right] \in \mathbb{R}^{n\times Nn}.
\end{aligned}$$

Then, one obtains

$$\begin{cases}
\hat{\varphi}(\dot{Q}(t)) = \hat{\varphi}\left(\chi\left(Q(t)\right)\right) + \hat{\varphi}\left(\vartheta\left(Q(t_k)\right)\right), & t \in [t_k, t_{k+1}), \\
\hat{\varphi}\left(Q(t_k)\right) = \hat{\varphi}\left(Q(t_k^-)\right).
\end{cases} \tag{6}$$

This expression can be simplified as

$$\begin{cases} \hat{\varphi}(\dot{Q}(t)) = A\hat{\varphi}\left(Q(t)\right) + B(\mathrm{e}^{\Lambda^{\mathrm{T}}h(t)} \otimes I_{m^2})\tilde{K}\hat{\varphi}\left(Q(t_k)\right), \quad t \in [t_k, t_{k+1}), \\ \hat{\varphi}\left(Q(t_k)\right) = \hat{\varphi}\left(Q(t_k^-)\right), \end{cases} \tag{7}$$

where

$$\begin{aligned} A &= \mathrm{diag}\left\{A_1 \oplus A_1, A_2 \oplus A_2, \ldots, A_N \oplus A_N\right\} + \Lambda^{\mathrm{T}} \otimes I_{n^2}, \\ B &= \mathrm{diag}\left\{B_1 \otimes B_1, B_2 \otimes B_2, \ldots, B_N \otimes B_N\right\}, \\ \tilde{K} &= \mathrm{diag}\left\{K_1 \otimes K_1, K_2 \otimes K_2, \ldots, K_N \otimes K_N\right\}, \\ \mathrm{e}^{\Lambda h(t)} &= \begin{bmatrix} p_{11}(h(t)) & p_{12}(h(t)) & \cdots & p_{1N}(h(t)) \\ p_{21}(h(t)) & p_{22}(h(t)) & \cdots & p_{2N}(h(t)) \\ \vdots & \vdots & \ddots & \vdots \\ p_{N1}(h(t)) & p_{N2}(h(t)) & \cdots & p_{NN}(h(t)) \end{bmatrix}. \end{aligned}$$

Because of $e_Q(t) = \hat{\varphi}\left(Q(t)\right) - \hat{\varphi}\left(Q(t_k)\right)$, one can easily obtain

$$\begin{cases} \hat{\varphi}(\dot{Q}(t)) = \bar{A}\hat{\varphi}\left(Q(t)\right) + B[(\mathrm{e}^{\Lambda^{\mathrm{T}}h(t)} + I_N) \otimes I_{m^2}]\tilde{K}\hat{\varphi}\left(Q(t)\right) - B(\mathrm{e}^{\Lambda^{\mathrm{T}}h(t)} \otimes I_{m^2})\tilde{K}e_Q(t), t \in [t_k, t_{k+1}), \\ \hat{\varphi}\left(Q(t_k)\right) = \hat{\varphi}\left(Q(t_k^-)\right), \end{cases} \tag{8}$$

where $\bar{A} = A - B\tilde{K}$.

Remark 1. Because of switching and state signals transmitted through networks, some unavoidable difficulties are encountered. First, because of the switching signal sampled, a mismatch phenomenon occurs between the original and sampled switching signals. Thus, many combinations of the original and sampled switching signals having up to $N \times N$ cases will occur and obviously lead to very large computational complexity. In particular, when the sampled switching signals are directly used to make system analysis and synthesis, many possible conditions are required, largely reducing the solvable solution set and even leading to no solution. Second, to solve the above-mentioned problems, a new model is developed by applying an auxiliary system approach, as described in (7) and (8). An additional term, namely $\mathrm{e}^{\Lambda^{\mathrm{T}}h(t)} \otimes I_{m^2}$, is introduced, which can be considered a novelly delayed system. When this term successfully describes the proposed problems, it also leads to larger difficulties and should be handled carefully. For example, the direct correlations among the auxiliary system state, the sampled error, and the upper bound of sampling intervals are not easily established. Third but not least, because the above new delay term is used rather than the usual delayed state, the conservatism is difficult to further reduce by applying a traditionally improved Lyapunov-Krasovsky function containing more delay information. The main reason is that the common methods for reducing the conservatism of delayed systems cannot be used to address the above exponential matrix directly and easily. Thus, more effects are needed to study this type of system.

Definition 2. If $\{t_k, k \in \mathbb{N}\}$ has a sampling lower bound $\underline{h}$ such that $h_k \geqslant \underline{h} > 0$, $k \in \mathbb{N}$, then it is considered a sample update sequence with a finite sampling rate property.

Definition 3. System (1) is said to be asymptotically mean square stable if there exist $x_0 \in \mathbb{R}^n$, $\eta_0 \in \mathscr{N}$, and its general solution $x(t, x_0)$ satisfies

$$\lim_{t\to\infty} \mathscr{E}\left[\|x(t, x_0, \eta_0)\|^2\right] = 0.$$

3 Main results

Theorem 1. A closed-loop control system is considered to be built from system (1) and control input (3), where $\tilde{K}$ is considered to satisfy $\bar{A} = A - B\tilde{K}$ and has negative real parts. This control system is asymptotically mean square stable under any control update sequence with a finite sampling rate if given scalars $\lambda > 0$ and $\rho > 0$, there exists a matrix $P > 0$ satisfying

$$\bar{A}^{\mathrm{T}}P + P\bar{A} < -\lambda I, \tag{9}$$

$$-\lambda+\beta_1\left(\beta_2+1\right)+\rho\beta_1\beta_2<0, \tag{10}$$

where $\beta_1=2\|PB\|\|\tilde{K}\|$ and $\beta_2=\mathrm{e}^{\|\Lambda\|\bar{h}}$. Furthermore, the sampling interval h_k, $\forall k\in\mathbb{N}$, should satisfy $h_k\leqslant\bar{h}$, which is computed as

$$\bar{h}=\frac{1}{\kappa_1}\frac{\rho}{1+\rho}, \tag{11}$$

where $\kappa_1=\|A\|+\beta_2\|B\|\|\tilde{K}\|$ when $\mu_A\leqslant 0$, and

$$\bar{h}=\frac{1}{\mu_A}\log\left[\left(\frac{\mu_A}{\kappa_1}\frac{\rho}{1+\rho}\right)+1\right], \tag{12}$$

when $\mu_A>0$.

Proof. The relevant Lyapunov function of (8) is described as

$$V(\hat{\varphi}\left(Q(t)\right),t)=\hat{\varphi}^{\mathrm{T}}\left(Q(t)\right)P\hat{\varphi}\left(Q(t)\right). \tag{13}$$

Then, it is obvious that

$$\alpha_1\|\hat{\varphi}\left(Q(t)\right)\|^2\leqslant V(\hat{\varphi}\left(Q(t)\right),t)\leqslant\alpha_2\|\hat{\varphi}\left(Q(t)\right)\|^2, \tag{14}$$

where α_1 and α_2 are the minimum and maximum eigenvalues of matrix P, respectively. On the basis of condition (9), one obtains

$$\begin{aligned}\dot{V}(\hat{\varphi}\left(Q(t)\right),t)=&\left\{\bar{A}\hat{\varphi}\left(Q(t)\right)+B\left[\left(\mathrm{e}^{\Lambda^{\mathrm{T}}h(t)}+I_N\right)\otimes I_{m^2}\right]\tilde{K}\hat{\varphi}\left(Q(t)\right)-B\left(\mathrm{e}^{\Lambda^{\mathrm{T}}h(t)}\otimes I_{m^2}\right)\tilde{K}e_Q(t)\right\}^{\mathrm{T}}\\&\times P\hat{\varphi}\left(Q(t)\right)+\hat{\varphi}^{\mathrm{T}}\left(Q(t)\right)P\left\{\bar{A}\hat{\varphi}\left(Q(t)\right)+B\left[\left(\mathrm{e}^{\Lambda^{\mathrm{T}}h(t)}+I_N\right)\otimes I_{m^2}\right]\tilde{K}\hat{\varphi}\left(Q(t)\right)\right.\\&\left.-B\left(\mathrm{e}^{\Lambda^{\mathrm{T}}h(t)}\otimes I_{m^2}\right)\tilde{K}e_Q(t)\right\}\\=&\,\hat{\varphi}^{\mathrm{T}}\left(Q(t)\right)\left(P\bar{A}\right)^{\star}\hat{\varphi}\left(Q(t)\right)+\hat{\varphi}^{\mathrm{T}}\left(Q(t)\right)\left\{PB\left[\left(\mathrm{e}^{\Lambda^{\mathrm{T}}h(t)}+I_N\right)\otimes I_{m^2}\right]\tilde{K}\right\}^{\star}\hat{\varphi}\left(Q(t)\right)\\&-e_Q^{\mathrm{T}}(t)\left[B\left(\mathrm{e}^{\Lambda^{\mathrm{T}}h(t)}\otimes I_{m^2}\right)\tilde{K}\right]^{\mathrm{T}}P\hat{\varphi}\left(Q(t)\right)-\hat{\varphi}^{\mathrm{T}}\left(Q(t)\right)PB\left(\mathrm{e}^{\Lambda^{\mathrm{T}}h(t)}\otimes I_{m^2}\right)\tilde{K}e_Q(t)\\\leqslant&-\lambda\|\hat{\varphi}\left(Q(t)\right)\|^2+\beta_1\left(\beta_2+1\right)\|\hat{\varphi}\left(Q(t)\right)\|^2+\beta_1\beta_2\|\hat{\varphi}\left(Q(t)\right)\|\|e_Q(t)\|,t\in[t_k,t_{k+1}).\end{aligned} \tag{15}$$

Furthermore,

$$\dot{V}(\hat{\varphi}\left(Q(t)\right),t)\leqslant-\lambda\|\hat{\varphi}\left(Q(t)\right)\|^2+\beta_1\left(\beta_2+1\right)\|\hat{\varphi}\left(Q(t)\right)\|^2+\beta_1\beta_2\|\hat{\varphi}\left(Q(t)\right)\|\|e_{\mathcal{Q}}(t)\|,t\in[t_k,t_{k+1}). \tag{16}$$

However, by substituting $e_Q(t)=\hat{\varphi}(Q(t))-\hat{\varphi}(Q(t_k))$, this expression can be rewritten as

$$\begin{cases}\dot{e}_Q(t)=&A\hat{\varphi}\left(Q(t)\right)+B\left(\mathrm{e}^{\Lambda^{\mathrm{T}}h(t)}\otimes I_{m^2}\right)\tilde{K}\hat{\varphi}\left(Q(t_k)\right),\ t\in[t_k,t_{k+1}),\\e_Q(t_k)=&0,\end{cases} \tag{17}$$

which is equal to

$$\begin{cases}\dot{e}_Q(t)=&A\hat{\varphi}\left(Q(t_k)\right)+Ae_Q(t)+B\left(\mathrm{e}^{\Lambda^{\mathrm{T}}h(t)}\otimes I_{m^2}\right)\tilde{K}\hat{\varphi}\left(Q(t_k)\right),\ t\in[t_k,t_{k+1}),\\e_Q(t_k)=&0.\end{cases} \tag{18}$$

Its solution is computed to be

$$\begin{aligned}e_Q(t)=&\,\mathrm{e}^{A(t-t_k)}e_Q(t_k)+\int_{t_k}^{t}\mathrm{e}^{A(t-s)}\left[A+B\left(\mathrm{e}^{\Lambda^{\mathrm{T}}h(t)}\otimes I_{m^2}\right)\tilde{K}\right]\hat{\varphi}\left(Q(t_k)\right)\mathrm{d}s\\=&\int_{t_k}^{t}\mathrm{e}^{A(t-s)}\left[A+B\left(\mathrm{e}^{\Lambda^{\mathrm{T}}h(t)}\otimes I_{m^2}\right)\tilde{K}\right]\hat{\varphi}\left(Q(t_k)\right)\mathrm{d}s\\\leqslant&\int_{t_k}^{t}\mathrm{e}^{\mu_A(t-s)}\left(\|A\|+\beta_2\|B\|\|\tilde{K}\|\right)\|\hat{\varphi}\left(Q(t_k)\right)\|\mathrm{d}s,t\in[t_k,t_{k+1}).\end{aligned} \tag{19}$$

Defining $f(t-t_k)=\int_{t_k}^{t}\mathrm{e}^{\mu_A(t-s)}\mathrm{d}s$ and considering $\hat{\varphi}(Q(t_k))=\hat{\varphi}(Q(t))-e_Q(t)$, it is known that

$$\|e_Q(t)\|\leqslant\kappa_1 f(t-t_k)\|e_Q(t)\|+\kappa_1 f(t-t_k)\|\hat{\varphi}\left(Q(t)\right)\|,\ t\in[t_k,t_{k+1}). \tag{20}$$

Obviously, it can be concluded that $f(t-t_k)$ monotonically increases with t and $f(0)=0$. For any positive real $h(t)$ such that

$$f(h(t))\leqslant\frac{1}{\kappa_1}\frac{\rho}{1+\rho},\ t\in[t_k,t_{k+1}), \tag{21}$$

it can be known that

$$\|e_Q(t)\|\leqslant\frac{\rho}{1+\rho}\|e_Q(t)\|+\frac{\rho}{1+\rho}\|\hat{\varphi}\left(Q(t)\right)\|,\ t\in[t_k,t_{k+1}). \tag{22}$$

Then, one obtains that

$$\|e_Q(t)\|\leqslant\rho\|\hat{\varphi}\left(Q(t)\right)\|,\ t\in[t_k,t_{k+1}). \tag{23}$$

Considering conditions (16) and (23), one obtains

$$\begin{aligned}\dot{V}(\hat{\varphi}\left(Q(t)\right),t)\leqslant&-\lambda\|\hat{\varphi}\left(Q(t)\right)\|^2+\left[\beta_1\left(\beta_2+1\right)+\rho\beta_1\beta_2\right]\|\hat{\varphi}\left(Q(t)\right)\|^2\\ \leqslant&-\delta\|\hat{\varphi}\left(Q(t)\right)\|^2,\ t\in[t_k,t_{k+1}),\end{aligned} \tag{24}$$

where $\delta=\lambda-[\beta_1(\beta_2+1)+\rho\beta_1\beta_2]\geqslant 0$. Therefore, it can be concluded that

$$\dot{V}(\hat{\varphi}\left(Q(t)\right),t)\leqslant-\delta\|\hat{\varphi}\left(Q(t)\right)\|^2\leqslant-\delta_1 V(\hat{\varphi}\left(Q(t)\right),t),\ t\in[t_k,t_{k+1}), \tag{25}$$

where $\delta_1=\delta/\alpha_2$. Thus, one can compute that

$$\begin{aligned}V(\hat{\varphi}\left(Q(t)\right),t)&\leqslant\mathrm{e}^{-\delta_1(t-t_k)}V(\hat{\varphi}\left(Q(t_k)\right),t)\\ &\leqslant\mathrm{e}^{-\delta_1(t-t_k)}V(\hat{\varphi}\left(Q(t_k^-)\right),t)\\ &\leqslant\mathrm{e}^{-\delta_1(t-t_k)}\mathrm{e}^{-\delta_1(t_k-t_{k-1})}V(\hat{\varphi}\left(Q(t_{k-1})\right),t)\\ &\vdots\\ &\leqslant\mathrm{e}^{-\delta_1 t}V(\hat{\varphi}\left(Q(0),t\right)),\ t\in[0,\infty).\end{aligned} \tag{26}$$

Then, one obtains

$$\|\hat{\varphi}\left(Q(t)\right)\|^2\leqslant\frac{\alpha_2}{\alpha_1}\mathrm{e}^{-\delta_1 t}\|\hat{\varphi}\left(Q(0)\right)\|^2,\ t\in[0,\infty), \tag{27}$$

which indicates that

$$\|\hat{\varphi}\left(Q(t)\right)\|\leqslant\sqrt{\frac{\alpha_2}{\alpha_1}}\mathrm{e}^{\frac{-\delta_1}{2}t}\|\hat{\varphi}\left(Q(0)\right)\|,\ t\in[0,\infty). \tag{28}$$

Because $\hat{\varphi}(Q(t))$ is derived from the linear transformation of $Q(t)$, $\lim_{t\to\infty}\|\hat{\varphi}(Q(t))\|=0$ obviously indicates that $\lim_{t\to\infty}\|Q(t)\|=0$. Because $Q_i(t)=\mathscr{E}[x(t)x^{\mathrm{T}}(t)\mathbb{1}_{\{\eta(t)=i\}}]$, one knows that

$$\begin{aligned}\lim_{t\to\infty}\mathscr{E}\left[\|x(t)\|^2\right]=&\lim_{t\to\infty}\sum_{i=1}^{N}\mathrm{tr}\left[\mathscr{E}\left[x(t)x^{\mathrm{T}}(t)\mathbb{1}_{\{\eta(t)=i\}}\right]\right]=\lim_{t\to\infty}\sum_{i=1}^{N}\mathrm{tr}\left[Q_i(t)\right]\\ \leqslant&\lim_{t\to\infty}n\sum_{i=1}^{N}\|Q_i(t)\|=\lim_{t\to\infty}n\|Q(t)\|_1=0.\end{aligned}$$

Therefore, the asymptotic stability of system (8) guarantees the asymptotically mean square stability of system (1). This completes the proof.

In Corollaries 1–7, more results of the special sampling situations of controller (3) are considered. When only $x(t)$ of traditional controller $u(t)=Kx(t)$ experiences sampling, it will be

$$u(t)=Kx(t_k),\ t\in[t_k,t_{k+1}). \tag{29}$$

In other words, controller (29) can be considered a mode-independent sampling controller. The resulting auxiliary system is simplified as

$$\hat{\varphi}\left(\dot{Q}(t)\right) = A\hat{\varphi}\left(Q(t)\right) + B\bar{K}\left(\mathrm{e}^{\Lambda^{\mathrm{T}}h(t)} \otimes I_{m^2}\right)\hat{\varphi}\left(Q(t_k)\right),\ t \in [t_k, t_{k+1}), \tag{30}$$

where $\bar{K} = \mathrm{diag}\{K \otimes K, K \otimes K, \ldots, K \otimes K\}$, and the other symbols are defined above. Then, one has the following corollary.

Corollary 1. A closed-loop control system is considered to be built from system (1) and control input (29), where $\bar{K}$ is considered to satisfy $\tilde{A} = A - B\bar{K}$ and has negative real parts. This control system is asymptotically mean square stable under any control update sequence with a finite sampling rate if given scalars $\lambda > 0$ and $\rho > 0$, there exists a matrix $P > 0$ satisfying

$$\tilde{A}^{\mathrm{T}}P + P\tilde{A} < -\lambda I, \tag{31}$$

$$-\lambda + \bar{\beta}_1\left(\beta_2 + 1\right) + \rho\bar{\beta}_1\beta_2 < 0, \tag{32}$$

where $\bar{\beta}_1 = 2\|PB\|\|\bar{K}\|$. Meanwhile, the upper sampling bound $\bar{h}$ can be computed as

$$\bar{h} = \frac{1}{\bar{\kappa}_1}\frac{\rho}{1+\rho}, \tag{33}$$

where $\bar{\kappa}_1 = \{\|A\| + \beta_2\|B\bar{K}\|\}$ when $\mu_A \leqslant 0$, and

$$\bar{h} = \frac{1}{\mu_A}\log\left[\left(\frac{\mu_A}{\bar{\kappa}_1}\frac{\rho}{1+\rho}\right) + 1\right] \tag{34}$$

when $\mu_A > 0$.

Proof. The proof is obtained similarly and omitted here. This completes the proof.

Remark 2. Note that Corollary 1 based on (29) is more conservative than Theorem 1 based on (3), although their conditions have similar forms. In detail, the conditions presented in this corollary can be obtained by specializing the parameters in this theorem when the parameter K_i in Theorem 1 is equal, that is, $K_1 = \cdots = K_N = K$. Thus, Corollary 1 is included in Theorem 1 as a special case with a smaller solvable set. In other words, controller (3), in which not only the state but also the switching signal is sampled, is better than controller (29), in which only the state is sampled. Consequently, more choices about controller (3) can be achieved, while only one mode selection about controller (29) obviously leads to more conservatism. Based on these facts and illustrations, the assertion can be made that the sampling of the switching signal is necessary and advantageous compared with the mode-independent sampled controller (29).

Second, when only switching signal $\eta(t)$ in (3) undergoes sampling, it will be

$$u(t) = K_{\eta(t_k)}x(t),\ t \in [t_k, t_{k+1}). \tag{35}$$

The resulting auxiliary system is simplified to be

$$\hat{\varphi}\left(\dot{Q}(t)\right) = A\hat{\varphi}\left(Q(t)\right) + B\left(\mathrm{e}^{\Lambda^{\mathrm{T}}h(t)} \otimes I_{m^2}\right)\tilde{K}\hat{\varphi}\left(Q(t)\right),\ t \in [t_k, t_{k+1}), \tag{36}$$

where the same symbols are defined above. Then, one will have the following corollary.

Corollary 2. A closed-loop control system is considered to be built from system (1) and control input (35), where $\tilde{K}$ is considered to satisfy $\bar{A}$ and have negative real parts. This control system is asymptotically mean square stable under any control update sequence with a finite sampling rate if given scalars $\lambda > 0$ and $\rho > 0$, there exists a matrix $P > 0$ satisfying conditions (9) and

$$-\lambda + \beta_1\left(\beta_2 + 1\right) \leqslant 0, \tag{37}$$

where the bound $\bar{h}$ can be selected to be a positive parameter satisfying condition (37).

Third, when only $x(t)$ in (3) undergoes sampling, it will be

$$u(t) = K_{\eta(t)}x(t_k),\ t \in [t_k, t_{k+1}). \tag{38}$$

This expression can be simplified as

$$\begin{cases} \hat{\varphi}(\dot{Q}(t)) = A\hat{\varphi}\left(Q(t)\right) + B\tilde{K}\left(\mathrm{e}^{\Lambda^{\mathrm{T}}h(t)} \otimes I_{m^2}\right)\hat{\varphi}\left(Q(t_k)\right),\ t \in [t_k, t_{k+1}), \\ \hat{\varphi}\left(Q(t_k)\right) = \hat{\varphi}\left(Q(t_k^-)\right). \end{cases} \tag{39}$$

Then, a corollary can be established.

Corollary 3. A closed-loop control system is considered to be built from system (1) and control input (38), where $\tilde{K}$ is considered to satisfy $\bar{A}$ and have negative real parts. This control system is asymptotically mean square stable under any control update sequence with a finite sampling rate if given scalars $\lambda > 0$ and $\rho > 0$, there exists a matrix $P > 0$ satisfying conditions (9) and

$$-\lambda + \tilde{\beta}_1\left(\beta_2 + 1\right) + \rho\tilde{\beta}_1\beta_2 < 0, \tag{40}$$

where $\tilde{\beta}_1 = 2\|PB\tilde{K}\|$, while the upper bound $\bar{h}$ is computed by

$$\bar{h} = \frac{1}{\tilde{\kappa}_1}\frac{\rho}{1+\rho}, \tag{41}$$

where $\tilde{\kappa}_1 = \{\|A\| + \beta_2\|B\tilde{K}\|\}$ when $\mu_A \leqslant 0$, and

$$\bar{h} = \frac{1}{\mu_A}\log\left[\left(\frac{\mu_A}{\tilde{\kappa}_1}\frac{\rho}{1+\rho}\right) + 1\right] \tag{42}$$

when $\mu_A > 0$.

Remark 3. On basis of the formulas for sampled controllers (35) and (38), Corollaries 2 and 3 can be considered less conservative than Theorem 1 closed by controller (3). The detailed reasons are given as follows: First, only the switching signal in controller (35) or only the system state signal in controller (38) is sampled, while both signals are sampled in controller (3). In other words, because the sampled signal is only an estimate of the original signal, it is natural that the effects based on controllers (35) and (38) are better than controller (3). Second, based on the given conditions, it can be concluded that Corollaries 2 and 3 are less conservative. In detail, compared with the conditions of Corollary 2, it is obvious that more constraints, such as positive term $\rho\beta_1\beta_2$, (11) and (12) with more parameter restrictions κ_1, and $\mu_A > 0$ or $\mu_A \leqslant 0$, are included in Theorem 1. The more conditions there are, the more conservative the results will be. However, investigating the conditions given in Corollary 3 and Theorem 1 reveals that they only differ in the computations of parameters β_1, $\tilde{\beta}_1$, κ_1, and $\tilde{\kappa}_1$. Particularly, the differences deeply depend on the computations of $\|PB\|\|\tilde{K}\|$ and $\|PB\tilde{K}\|$. Obviously, $\|PB\tilde{K}\|$ is better than $\|PB\|\|\tilde{K}\|$ in terms of leading to less conservatism. Third, the superiorities of Corollaries 2 and 3 over Theorem 1 in terms of less conservatism will be shown using a numerical example.

Particularly, some traditional controllers for MJSs are considered by using the main methods in this paper. A mode-dependent controller is presented as follows:

$$u(t) = K_{\eta(t)}x(t),\ t \in [0, \infty), \tag{43}$$

whose auxiliary system is

$$\hat{\varphi}\left(\dot{Q}(t)\right) = A\hat{\varphi}\left(Q(t)\right) + B\tilde{K}\hat{\varphi}\left(Q(t)\right). \tag{44}$$

Then, the following corollary can be obtained.

Corollary 4. A closed-loop control system is considered to be built from system (1) and control input (43), and it is asymptotically mean square stable if given a scalar $\lambda > 0$, there exists a matrix $P > 0$ satisfying

$$\hat{A}^{\mathrm{T}}P + P\hat{A} < -\lambda I, \tag{45}$$

where $\hat{A} = A + B\tilde{K}$.

Alternatively, a mode-independent controller is expressed as

$$u(t) = Kx(t),\ t \in [0, \infty), \tag{46}$$

whose auxiliary system is

$$\hat{\varphi}\left(\dot{Q}(t)\right) = A\hat{\varphi}\left(Q(t)\right) + B\bar{K}\hat{\varphi}\left(Q(t)\right). \tag{47}$$

Similarly, one has the following corollary.

Corollary 5. A closed-loop control system is considered to be built from system (1) and control input (46), and it is asymptotically mean square stable if given a scalar $\lambda > 0$, there exists a matrix $P > 0$ satisfying

$$\check{A}^{\mathrm{T}}P + P\check{A} < -\lambda I, \tag{48}$$

where $\check{A} = A + B\bar{K}$.

Remark 4. It can be claimed that Corollary 2 based on controller (35) is better than Corollary 5 based on controller (46) in terms of having less conservatism. The phenomenon is similar to the comparisons between controllers (3) and (29), which is also illustrated in Remark 2. The main reasons are summarized as follows: On the one hand, more selections of control gain are provided in the former controller, although its switching is sampled. In other words, when all the control gains of (35) are selected to be a common one, it will be reduced to controller (46); on the other hand, the superiority of controller (35) over controller (46) will be demonstrated using a numerical example.

Remark 5. Based on the explanations in the above remarks, except for Remark 1, it can be concluded that mode-dependent controller (43) without any sampling has less conservatism than sampled controllers (3), (35), and (38), where switching and/or state signals are sampled. Similarly, mode-independent controller (46) without sampling is also less conservative than mode-independent but sampled controller (29). Although controllers (43) and (46) have less conservatism than the abovementioned controllers, they have smaller application scopes. In detail, the variables in such traditionally mode-dependent and mode-independent controllers should be assumed to be available online. This availability is obviously impossible when such signals are transmitted through communication networks. Thus, all the proposed problems in this paper are meaningful, and which of them to be used should be considered in actual situations.

Last but not least, another special situation of a scalar system is proposed as

$$\mathrm{d}x(t) = a_{\eta(t)}x(t)\mathrm{d}t + \sigma_{\eta(t_k)}x(t_k)\mathrm{d}\omega(t), \tag{49}$$

where $a_{\eta(t)}$ and $\sigma_{\eta(t_k)}$ are scalars. Similar to system (5), one obtains that

$$\mathrm{d}q_i(t) = 2a_iq_i(t)\mathrm{d}t + \sum_{j=1}^{N}\lambda_{ji}q_j(t)\mathrm{d}t + \sum_{\ell=1}^{N}p_{\ell i}\left(h(t)\right)\sigma_\ell^2 q(t_k)\mathrm{d}t, \tag{50}$$

where $q_i(t)$ is defined similar to $Q_i(t)$ but referred to as scalar $x(t)$ instead of vector $x(t)$. It is rewritten as

$$\dot{q}(t) = aq(t) + \mathrm{e}^{\Lambda^{\mathrm{T}}h(t)}\sigma q(t_k),\quad t \in [t_k, t_{k+1}), \tag{51}$$

where

$$q(t) = \left[\begin{array}{ccc} q_1(t) & \cdots & q_N(t) \end{array}\right]^{\mathrm{T}},\quad a = \mathrm{diag}\left\{2a_1, \ldots, 2a_N\right\} + \Lambda^{\mathrm{T}},\quad \sigma = \mathrm{diag}\left\{\sigma_1^2, \ldots, \sigma_N^2\right\}.$$

Because $e_q(t) = q(t) - q(t_k)$, it is equal to

$$\dot{q}(t) = \bar{a}q(t) + \left(\mathrm{e}^{\Lambda^{\mathrm{T}}h(t)} + I_N\right)\sigma q(t) - \mathrm{e}^{\Lambda^{\mathrm{T}}h(t)}\sigma e_q(t),\quad t \in [t_k, t_{k+1}), \tag{52}$$

where $\bar{a} = a + \Lambda^{\mathrm{T}} - \sigma$. Then, one has the following corollary.

Corollary 6. Consider the control system (49), where all eigenvalues of $\bar{a}$ have negative real parts. This control system is asymptotically mean square stable under any control update sequence with a finite sampling rate if given scalars $\lambda > 0$ and $\rho > 0$, there exists a matrix $P > 0$ satisfying

$$\bar{a}^{\mathrm{T}}P + P\bar{a} < -\lambda I, \tag{53}$$

$$-\lambda+\hat{\beta}_1\left(\beta_2+1\right)+\rho\hat{\beta}_1\beta_2<0, \tag{54}$$

where $\hat{\beta}_1=2\|P\|\|\sigma\|$. At the same time, the upper bound $\bar{h}$ of sampling is calculated as

$$\bar{h}=\frac{1}{\hat{\kappa}_1}\frac{\rho}{1+\rho}, \tag{55}$$

where $\hat{\kappa}_1=\|a\|+\beta_2\|\sigma\|$ when $\mu_a\leqslant 0$, and

$$\bar{h}=\frac{1}{\mu_a}\log\left[\left(\frac{\mu_a}{\hat{\kappa}_1}\frac{\rho}{1+\rho}\right)+1\right] \tag{56}$$

when $\mu_a>0$.

Proof. The proof is similar to the proof of Theorem 1 and is omitted here. This completes the proof.

Furthermore, when the sampling interval of system (49) is constant, it can be studied by introducing the following system:

$$\mathrm{d}x(t)=a_{\eta(t)}x(t)\mathrm{d}t+\sigma_{\eta(\delta_t)}x(\delta_t)\mathrm{d}\omega(t), \tag{57}$$

where $\delta_t=[\frac{t}{\tau}]\tau$ is the integer part of t/τ, and τ is the constant sampling range. Notably, when there is no jump in system (57), it will be reduced to the one considered in [12]. In detail, the stability was considered in terms of almost certain exponential stability. Based on the key idea of this reference and exploiting improved and novel techniques, similar results are obtained as follows.

Corollary 7. Considering control system (57), it can be almost surely exponentially stable for any τ satisfying $\tau\in(0,\bar{\tau})$ that

$$\limsup_{t\to\infty}\frac{1}{t}\log\left(|x(t)|\right)<0\quad\text{a.s.},$$

if given a constant $\varepsilon>0$, there exists $r_i>0$ satisfying

$$2r_ia_i+\sigma_\ell^2+\sum_{j=1}^{N}\lambda_{ij}r_j<0,\quad\forall i,\ell\in\mathscr{N}. \tag{58}$$

Meanwhile, the upper bound $\bar{\tau}$ is the unique root of the following equation:

$$\frac{\bar{\alpha}_1}{\bar{\alpha}_2}\varepsilon+4\mathcal{G}_{\bar{\tau}}\left[\mathrm{e}^{\left(4\bar{\alpha}_1+3\gamma^2\right)\left(\bar{\tau}+\frac{\log(4/\varepsilon)}{\beta}\right)}-1\right]=1, \tag{59}$$

where $\bar{\alpha}_1=\max_{i\in\mathscr{N}}\{|a_i|\}$, $\bar{\alpha}_2=\min_{i\in\mathscr{N}}\{|a_i|\}$, $\mathcal{G}_{\bar{\tau}}=\frac{4\gamma^2(\bar{\alpha}_1\bar{\tau}^2+\gamma^2\bar{\tau})}{2\bar{\alpha}_1+\gamma^2}$, $\gamma=\max_{\ell\in\mathscr{N}}\{|\sigma_\ell|\}$, $\beta=-\frac{\varsigma}{\bar{\alpha}_2}$, and $\varsigma=\max_{i,\ell\in\mathscr{N}}\{2r_ia_i+\sigma_\ell^2+\sum_{j=1}^{N}\lambda_{ij}r_j\}$.

Proof. The proof is similar to the one given in [12] and is omitted here. This completes the proof.

Remark 6. Although Corollaries 6 and 7 are proposed for studying system (49) under constant sampling, they are obtained by applying different techniques. The former corollary is based on the auxiliary system approach and fully considers the sampling error, while the latter corollary is established using a robust estimation method [12, 33]. As mentioned in Section 1, parameter τ should be very small and constant. In this situation, the larger the value of τ is, the better the performance and the less the conservatism. In Section 4, some numerical examples will be used to compare such corollaries, which will demonstrate our methods better.

Remark 7. Similar to the corollaries proposed above, some extensions of special controllers for (49) can be easily and directly presented and are omitted.

4 Numerical example

Example 1. Consider a system of form (1) whose matrices are described as

$$A_1=\begin{bmatrix}-2 & 0.1\\ 0.1 & 0\end{bmatrix},\ A_2=\begin{bmatrix}0+\delta & 0.1\\ 3.1 & -2\end{bmatrix},\ B_1=\begin{bmatrix}0.1\\ 0.2\end{bmatrix},\ B_2=\begin{bmatrix}0.2\\ 0.1\end{bmatrix},$$

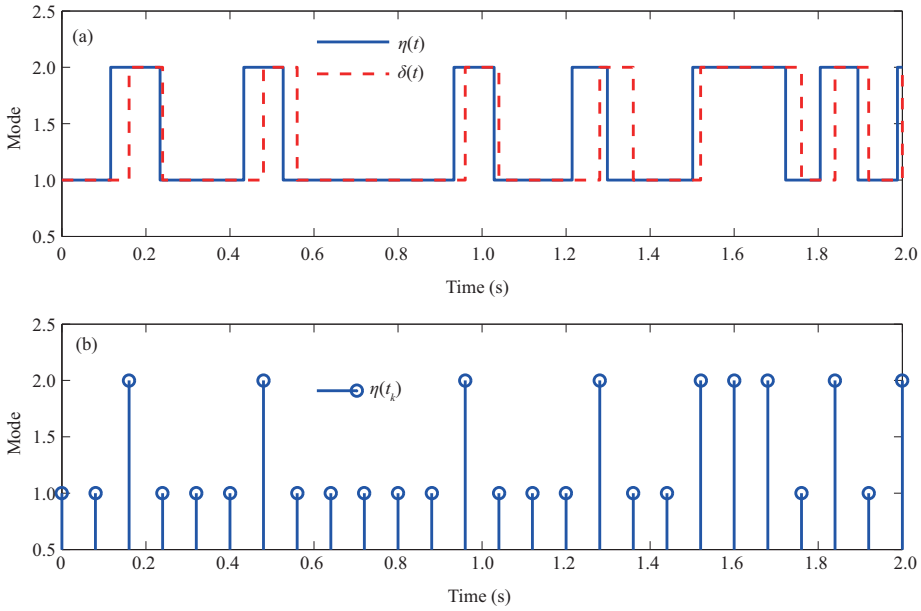

Figure 2 (Color online) Simulations of signals $\eta(t)$, $\delta(t)$, and $\eta(t_k)$.

where $\delta \geqslant 0$ is assumed to be a disturbance and will be used for comparisons. Obviously, there are two modes, that is, $\eta(t) \in \mathscr{N} = \{1, 2\}$, whose transition rate matrix is given as

$$\Pi = \begin{bmatrix} -2 & 2 \\ 3 & -3 \end{bmatrix}.$$

Without losing generality, it is assumed that the gains of controller (3) are given as follows: $K_1 = [\,-1.5 \;\; 0.6\,]$ and $K_2 = [\,0.8 \;\; -0.8\,]$. Without losing generality, letting $\lambda = 0.4$, it can be computed from Theorem 1 with $\delta = 0$ that $P = \mathrm{diag}\{P_1, P_2\}$, where P_1 and P_2 are computed to be

$$P_1 = \begin{bmatrix} 0.1658 & 0.0054 & 0.0054 & -0.0036 \\ 0.0054 & 0.2235 & 0.0019 & 0.0136 \\ 0.0054 & 0.0019 & 0.2235 & 0.0136 \\ -0.0036 & 0.0136 & 0.0136 & 0.4025 \end{bmatrix}, \quad P_2 = \begin{bmatrix} 0.2840 & 0.0080 & 0.0080 & -0.0015 \\ 0.0080 & 0.1854 & 0.0015 & 0.0067 \\ 0.0080 & 0.0015 & 0.1854 & 0.0067 \\ -0.0015 & 0.0067 & 0.0067 & 0.1737 \end{bmatrix}.$$

Furthermore, the upper bound $\bar{h}$ of sampling interval h_k, $\forall k \in \mathbb{N}$, is computed as $\bar{h} = 0.0718$. Particularly, for the simulations of the original switching signal $\eta(t)$, its sampled signal $\eta(t_k)$, and its ZOH signal $\delta(t)$, denoted by $\delta(t)$, are given in Figure 2. Moreover, under the initial condition $x_0 = [\,-1 \;\; 1\,]^{\mathrm{T}}$ and applying the above-designed controller, one has the curves of the closed-loop system shown in Figure 3. On the basis of this simulation, although the switching and state signals experience sampling phenomena, the usefulness of the presented controller is nonetheless apparent. Next, the main results, such as theorems and corollaries, will be compared. First, comparisons between Theorem 1 and Corollary 1 will be made, where parameter λ in this corollary is selected to be $\lambda = 0.4$. Meanwhile, without losing generality, the gain of controller (29) is selected to be $K = [\,-1.5 \;\; 0.6\,]$, which is similar to mode-independent situations [22,23]. Then, the upper sampling bounds of Theorem 1 and Corollary 1 are given in Table 1. To illustrate the comparisons vividly, the correlations between disturbance δ and maximum allowable $\bar{h}$ are simulated in Figure 4(a). On the basis of these comparisons and simulations, Theorem 1 is found to be better than Corollary 1, where the theorem could suffer a larger sampling bound for the same disturbance. In other words, the strategy based on Theorem 1 could reduce the burden of the communication network because a larger sampling interval could be borne.

Under identical controller gains K_1 and K_2, similar comparisons and simulations between Theorem 1 and Corollary 2 are made in Table 2 and Figure 4(b). At the same time, more comparisons between

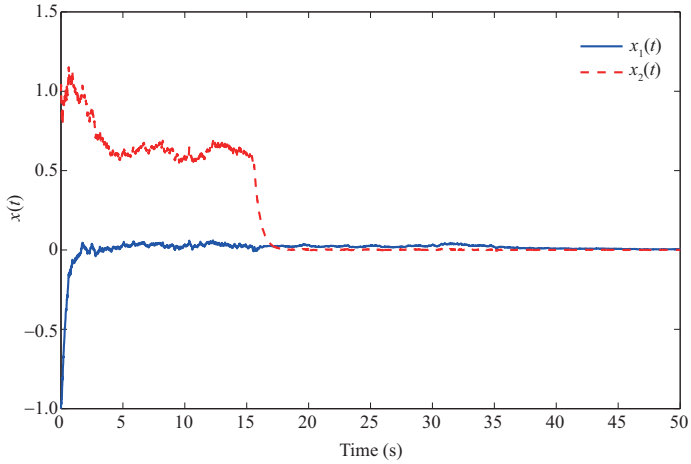

Figure 3 (Color online) State response of the closed-loop system by controller (3).

Table 1 Comparisons of the $\bar{h}$ of Theorem 1 and Corollary 1 along with δ

	δ											
	0	0.1	0.2	0.3	0.4	0.5	0.6	0.7	0.8	0.9	1	1.1
Theorem 1	0.0718	0.0706	0.0704	0.0694	0.0686	0.0654	0.0643	0.0528	0.0335	0.0281	0.0177	–
Corollary 1	0.0531	0.0510	0.0485	0.0462	0.0440	0.0417	0.0394	0.0352	0.0312	–	–	–

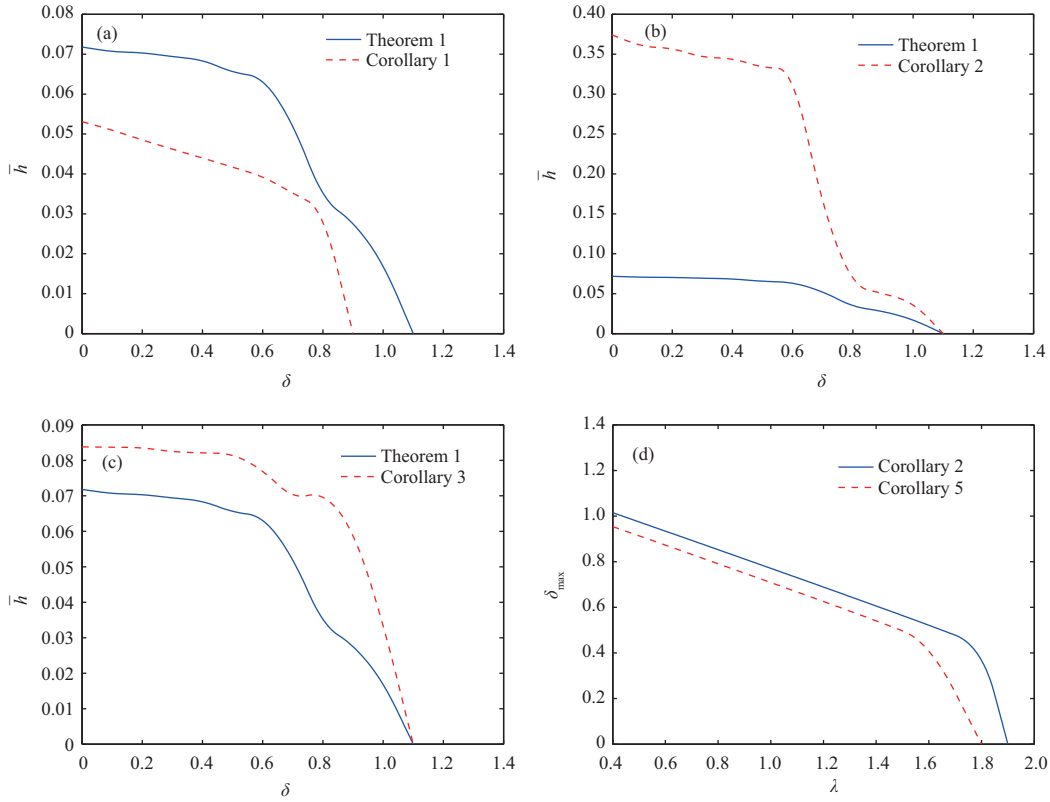

Figure 4 (Color online) Comparison simulations of (a) Theorem 1 and Corollary 1; (b) Theorem 1 and Corollary 2; (c) Theorem 1 and Corollary 3; (d) Corollary 2 and Corollary 5.

Theorem 1 and Corollary 3 and the corresponding simulations are provided in Table 3 and Figure 4(c), respectively. These comparisons are shown to support the statements presented in Remark 3 very well.

Next, more comparisons between Corollary 2 and Corollary 5 will be made, where the control gain in the latter corollary is given as $K = [\,-1.5 \;\; 0.6\,]$. Then, similar comparisons and simulations of the δ of such

Table 2 Comparisons of the $\bar{h}$ of Theorem 1 and Corollary 2 along with δ

	δ											
	0	0.1	0.2	0.3	0.4	0.5	0.6	0.7	0.8	0.9	1	1.1
Theorem 1	0.0718	0.0706	0.0704	0.0694	0.0686	0.0654	0.0643	0.0528	0.0335	0.0281	0.0177	–
Corollary 2	0.3741	0.3594	0.3576	0.3459	0.3449	0.3330	0.3317	0.1566	0.0588	0.0504	0.0390	–

Table 3 Comparisons of the $\bar{h}$ of Theorem 1 and Corollary 3 along with δ

	δ											
	0	0.1	0.2	0.3	0.4	0.5	0.6	0.7	0.8	0.9	1	1.1
Theorem 1	0.0718	0.0706	0.0704	0.0694	0.0686	0.0654	0.0643	0.0528	0.0335	0.0281	0.0177	–
Corollary 3	0.0838	0.0837	0.0836	0.0824	0.0821	0.0819	0.0773	0.0691	0.0711	0.0607	0.0343	–

Table 4 Comparisons on $\delta_{\max}$ of Corollary 2 and Corollary 5 along with λ

	λ									
	0.4	0.6	0.8	1.0	1.1	1.2	1.4	1.6	1.8	1.9
Corollary 2	1.015	0.934	0.853	0.771	0.730	0.689	0.606	0.522	0.434	0
Corollary 5	0.954	0.873	0.791	0.709	0.667	0.626	0.541	0.453	0	0

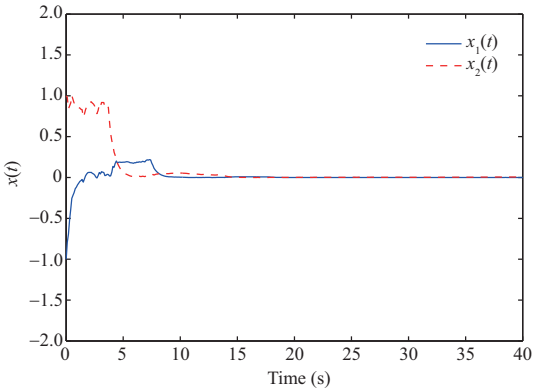

Figure 5 (Color online) Simulation of the closed-loop system by controller (43).

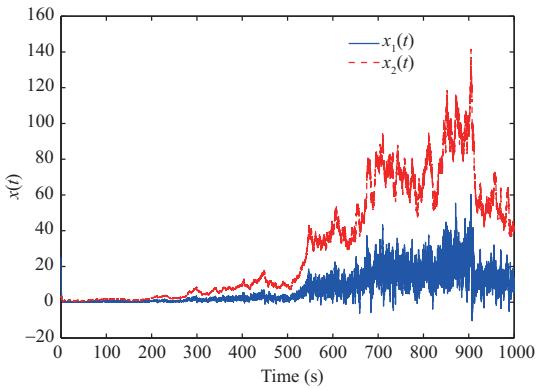

Figure 6 (Color online) Simulation of controller (43) experiencing the sampling effect.

corollaries are obtained in Table 4 and Figure 4(d), respectively, where $\delta_{\max}$ is the maximum allowable value of δ. On the basis of these comparisons, Corollary 2 is better than Corollary 5 in terms of having less conservatism, in which the former corollary can bear a larger disturbance. The main reason is that more controllers based on Corollary 2 can be designed, although there exists a sampling phenomenon.

Finally, explanations and simulations about Corollaries 4 and 5 will be given. Without losing generality, only Corollary 4 is mentioned here, while Corollary 5 could be addressed similarly and is omitted. Based on the illustrations in Remark 5, it is known that controller (43) based on Corollary 4 is less conservative, but its assumption about switching and state signals is ideal. Thus, the information should be exactly available in real time. Moreover, this constraint is sometimes difficult or impossible to satisfy. In other words, when the above assumption about controller (43) is not satisfied, the ideal controller (43), whose phenomenon is illustrated as follows, will be disabled. Without losing generality, the gains of controller (43) similar to those in [18–21] are selected as $K_1 = [\,0.8\ -0.6\,]$ and $K_2 = [\,0.8\ -2\,]$, where $\lambda = 0.4$. On the basis of Corollary 4, the resulting system is known to be stable, and the state simulations are given in Figure 5. However, when the above controller experiences the above sampling effect illustrated in Figure 2, the closed-loop system will be unstable, and the stabilizing effect is demonstrated in Figure 6. Obviously, it is unstable and shows the statements in Remark 5.

Example 2. Consider a scalar system (49) with three modes, $\eta(t) \in \mathscr{N} = \{1, 2, 3\}$, whose parameters are given as (Mode 1) $a_1 = 0.1$, $\sigma_1 = -0.08$; (Mode 2) $a_2 = 0.2$, $\sigma_2 = 0.05$; and (Mode 3) $a_3 = -3$,

Table 5 Maximum allowable bounds of sampling under different σ_3 values

	σ_3									
	0.09	0.11	0.13	0.15	0.17	0.19	0.21	0.23	0.25	0.27
$\bar{h}$	0.09473	0.08919	0.08299	0.07592	0.06803	0.05942	0.04991	0.03959	0.02793	0.01581
$\bar{\tau}$	0.03149	0.02502	0.02018	0.01634	0.01317	0.01052	0.00830	0.00646	0.00498	0.00380

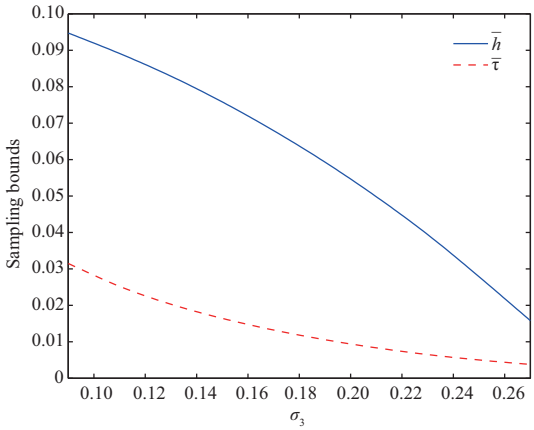

Figure 7 (Color online) Comparison simulations of Corollaries 6 and 7.

$\sigma_3 = 0.09$. Its transition rate matrix is given as

$$\Pi = \begin{bmatrix} -5 & 3 & 2 \\ 0 & -5 & 5 \\ 1 & 1 & -2 \end{bmatrix}.$$

Without losing generality, letting $\rho = 8.92$ and $\lambda = 0.4$, it can be computed from Corollary 6 that $P_1 = 1.1728$, $P_2 = 0.9488$, and $P_3 = 0.8503$, where the upper bound of sampling is $\bar{h} = 0.09473$. Meanwhile, based on Corollary 7, one obtains $r_1 = 1.6736$, $r_2 = 1.3500$, and $r_3 = 0.7120$, where the upper bound is $\bar{\tau} = 0.03149$. Obviously, the former upper bound is larger than the latter upper bound. Then, it can be said that our methods are less conservative than the ones based on [12]. To further demonstrate the superiority of our methods, more comparisons are made as follows. On the basis of the conditions presented in Corollaries 6 and 7, upper bounds $\bar{h}$ and $\bar{\tau}$ are known to be affected by $\max_{\eta(t)\in\mathcal{N}}\{|\sigma_{\eta(t)}|\}$. Therefore, more comparisons between such corollaries can be obtained by only changing the value of σ_3 given in Table 5, whose correlations between $\bar{h}$ and $\bar{\tau}$ under identical conditions can be established. Moreover, to illustrate the comparisons vividly, some simulations are given in Figure 7. On the basis of these comparisons and simulations, the methods proposed in this paper are seen to have advantages over the method in [12], in which larger sampling bounds are allowed. In other words, by allowing a larger sampling interval, the performance and efficiency of communication networks can be improved.

5 Conclusion

In this study, the stabilizing control problem of continuous time MJSs in which not only the state but also the switching signal is sampled was investigated by applying an auxiliary system approach. A new model having an exponential matrix was proposed to characterize the sampling effects and overcome the difficulties coming from sampled signals. Sufficient conditions were given to depend deeply on the sampling rate. More special extensions were separately considered, where comparisons were made to illustrate the advantages of the methods in this paper. Finally, more difficult problems still need to be studied. First, when there is a time delay in system (1), the problems will be very complicated and difficult. The main reason is that delay brings large negative effects when a Markovian switching signal suffers sampling. Second, the conservatism must be reduced because enlarged inequalities and techniques are introduced. Third but not least, only asymptotical mean square stability was studied here. When

other stability concepts are mentioned, whether the auxiliary system approach is suitable should be revisited.

Acknowledgements This work was supported by Open Project of Key Field Alliance of Liaoning Province (Grant No. 2022-KF-11-03), and National Natural Science Foundation of China (Grant Nos. 61903076, 62073158). The authors would like to thank the anonymous associate editor and reviewers for their very helpful comments and suggestions.

References

1 Zhang W, Branicky M S, Phillips S M. Stability of networked control systems. IEEE Control Syst Mag, 2001, 21: 84–99
2 Zhang L X, Gao H J, Kaynak O. Network-induced constraints in networked control systems—a survey. IEEE Trans Ind Inf, 2013, 9: 403–416
3 Qi W, Zong G, Karimi H R. $\mathscr{L}_\infty$ control for positive delay systems with semi-Markov process and application to a communication network model. IEEE Trans Ind Electron, 2019, 66: 2081–2091
4 Xie L, Xie L H. Stability analysis of networked sampled-data linear systems with Markovian packet losses. IEEE Trans Automat Contr, 2009, 54: 1375–1381
5 Luo Q, Gong Y Y, Jia C X. Stability of gene regulatory networks with Lévy noise. Sci China Inf Sci, 2017, 60: 072204
6 Peng C, Sun H. Switching-like event-triggered control for networked control systems under malicious denial of service attacks. IEEE Trans Automat Contr, 2020, 65: 3943–3949
7 Guo L, Cui T T, Yu H, et al. Stability of networked control system subject to denial-of-service. Sci China Inf Sci, 2021, 64: 129203
8 Zhou W, Fu J, Yan H, et al. Event-triggered approximate optimal path-following control for unmanned surface vehicles with state constraints. IEEE Trans Neural Netw Learn Syst, 2023, 34: 104–118
9 Chen W M, Xu S Y, Zou Y. Stabilization of hybrid neutral stochastic differential delay equations by delay feedback control. Syst Control Lett, 2016, 88: 1–13
10 Mao W H, Deng F Q, Wan A H. Robust H_2/H_∞ global linearization filter design for nonlinear stochastic time-varying delay systems. Sci China Inf Sci, 2016, 59: 032204
11 Li X Y, Mao X. Stabilisation of highly nonlinear hybrid stochastic differential delay equations by delay feedback control. Automatica, 2020, 112: 108657
12 Mao X. Almost sure exponential stabilization by discrete-time stochastic feedback control. IEEE Trans Automat Contr, 2016, 61: 1619–1624
13 Costa O L V, Fragoso M D, Todorov M G. Continuous-Time Markov Jump Linear Systems. Berlin: Springer, 2012
14 Wang Y, Pu H, Shi P, et al. Sliding mode control for singularly perturbed Markov jump descriptor systems with nonlinear perturbation. Automatica, 2021, 127: 109515
15 Wang G L, Xu L. Almost sure stability and stabilization of Markovian jump systems with stochastic switching. IEEE Trans Automat Contr, 2022, 67: 1529–1536
16 Shen H, Hu X H, Wang J, et al. Non-fragile H_∞ synchronization for Markov jump singularly perturbed coupled neural networks subject to double-layer switching regulation. IEEE Trans Neural Netw Learn Syst, 2023, 34: 2682–2692
17 Shen H, Xing M P, Yan H C, et al. Observer-based l_2-l_∞ control for singularly perturbed semi-Markov jump systems with an improved weighted TOD protocol. Sci China Inf Sci, 2022, 65: 199204
18 Shen H, Li F, Xu S, et al. Slow state variables feedback stabilization for semi-Markov jump systems with singular perturbations. IEEE Trans Automat Contr, 2017, 63: 2709–2714
19 Jiang B, Kao Y G, Karimi H R, et al. Stability and stabilization for singular switching semi-Markovian jump systems with generally uncertain transition rates. IEEE Trans Automat Contr, 2018, 63: 3919–3926
20 Qi W, Zong G, Karim H R. Observer-based adaptive SMC for nonlinear uncertain singular semi-Markov jump systems with applications to DC motor. IEEE Trans Circuits Syst I, 2018, 65: 2951–2960
21 Wang Y Y, Xia Y Q, Shen H, et al. SMC design for robust stabilization of nonlinear Markovian jump singular systems. IEEE Trans Automat Contr, 2017, 63: 219–224
22 de Souza C E, Trofino A, Barbosa K A. Mode-independent H_∞ filters for Markovian jump linear systems. IEEE Trans Automat Contr, 2006, 51: 1837–1841
23 Liu P H, Ho D W C, Sun F C. Design of H_∞ filter for Markov jumping linear systems with non-accessible mode information. Automatica, 2008, 44: 2655–2660
24 Wang G L, Li B Y, Zhang Q L, et al. A partially delay-dependent and disordered controller design for discrete-time delayed systems. Int J Robust Nonlinear Control, 2017, 27: 2646–2668
25 Costa O L V, Fragoso M D, Todorov M G. A detector-based approach for the H_2 control of Markov jump linear systems with partial information. IEEE Trans Automat Contr, 2014, 60: 1219–1234
26 Wang G L, Zhang Q L, Yang C Y. Fault-tolerant control of Markovian jump systems via a partially mode-available but unmatched controller. J Franklin Inst, 2017, 354: 7717–7731
27 Wang G L, Sun Y Y. Almost sure stabilization of continuous-time jump linear systems via a stochastic scheduled controller. IEEE Trans Cybern, 2022, 52: 2712–2724

28 Wang G L. Stabilization of semi-Markovian jump systems via a quantity limited controller. Nonlinear Anal-Hybrid Syst, 2021, 42: 101085

29 Mao X, Yin G, Yuan C. Stabilization and destabilization of hybrid systems of stochastic differential equations. Automatica, 2007, 43: 264–273

30 Deng F Q, Luo Q, Mao X. Stochastic stabilization of hybrid differential equations. Automatica, 2012, 48: 2321–2328

31 Huang L R. Stochastic stabilization and destabilization of nonlinear differential equations. Syst Control Lett, 2013, 62: 163–169

32 Song G F, Lu Z Y, Zheng B-C, et al. Almost sure stabilization of hybrid systems by feedback control based on discrete-time observations of mode and state. Sci China Inf Sci, 2018, 61: 070213

33 Mao X. Stabilization of continuous-time hybrid stochastic differential equations by discrete-time feedback control. Automatica, 2013, 49: 3677–3681

34 Xiao X Q, Zhou L, Ho D W C, et al. Event-triggered control of continuous-time switched linear systems. IEEE Trans Automat Contr, 2018, 64: 1710–1717

35 Chen G, Sun J, Chen J. Mean square exponential stabilization of sampled-data Markovian jump systems. Int J Robust Nonlinear Control, 2018, 28: 5876–5894

36 Chen G, Sun J, Chen J. Passivity-based robust sampled-data control for Markovian jump systems. IEEE Trans Syst Man Cybern Syst, 2020, 50: 2671–2684

37 Wu X, Mu X. H_∞ stabilization for networked semi-Markovian jump systems with randomly occurring uncertainties via improved dynamic event-triggered scheme. Int J Robust Nonlinear Control, 2019, 29: 4609–4626

38 Wan H Y, Luan X L, Karimi H R, et al. Dynamic self-triggered controller codesign for Markov jump systems. IEEE Trans Automat Contr, 2020, 66: 1353–1360

39 Zeng P Y, Deng F Q, Liu X H, et al. Event-triggered resilient $\mathscr{L}_\infty$ control for Markov jump systems subject to denial-of-service jamming attacks. IEEE Trans Cybern, 2022, 52: 10240–10252

40 Cao Z, Niu Y, Song J. Finite-time sliding-mode control of Markovian jump cyber-physical systems against randomly occurring injection attacks. IEEE Trans Automat Contr, 2019, 65: 1264–1271